Selective Photooxidation of Small Alkenes by O_2 with Red Light in Zeolite Y

Fritz Blatter and Heinz Frei*

Contribution from the Laboratory of Chemical Biodynamics, Lawrence Berkeley Laboratory, University of California, Berkeley, California 94720

*Received October 12, 1993. Revised Manuscript Received December 30, 1993**

Abstract: Upon loading of 2,3-dimethyl-2-butene (DMB) and O_2 into zeolite NaY, photochemistry was observed at wavelengths as long as 760 nm. Similarly, photoexcitation of *trans*- or *cis*-2-butene and O_2 in this zeolite resulted in chemical reaction at a threshold wavelength of 600 nm. Reactions were initiated either with filtered tungsten-source light or the emission of a CW dye laser and typically conducted at −50 °C. Products identified by FT-infrared spectroscopy were 2,3-dimethyl-3-hydroperoxy-1-butene (>90%) and acetone in the case of DMB + O_2. *trans*- or *cis*-2-butene + O_2 gave exclusively 3-hydroperoxy-1-butene. This constitutes the first synthesis of this hydroperoxide by direct photolysis of 2-butene·O_2 pairs. Laser reaction excitation spectra in the 500–700-nm region revealed a continuous absorption for both the DMB·O_2 and the 2-butene·O_2 systems. It is attributed to a charge-transfer transition. Comparison with corresponding absorption spectra in conventional media shows that the excited alkene·O_2 charge-transfer states are stabilized by electrostatic interactions with the zeolite NaY environment by 12 000 cm^{-1}. Substantially less stabilization was observed in high-silica faujasite. Thermal decomposition of the hydroperoxide photoproducts upon warm-up from −50 °C to room temperature was monitored by infrared spectroscopy. It was found that 3-hydroperoxy-1-butene thermally epoxidizes the excess *cis*- or *trans*-2-butene in room temperature NaY under complete stereochemical retention.

I. Introduction

Selective oxidation of small abundant hydrocarbons is the most important type of reaction in organic chemicals production. For example, essentially all building blocks for the manufacture of plastics and synthetic fibers are produced by oxidation of hydrocarbons.[1] Among these, oxidations by molecular oxygen play a particularly important role.[2] A key problem is the product specificity in hydrocarbon + O_2 reactions, and here photoassisted processes hold special promise. Photoinitiated reactions of O_2 furnish access to products that in many cases cannot be obtained by a dark reaction of O_2. Moreover, photochemical reactions can be conducted at or around ambient temperature, thus minimizing the chance for loss of product specificity due to secondary thermal chemistry of the initial product(s) (rearrangement, fragmentation, bimolecular reactions).

There are three well-established types of hydrocarbon photooxidation reactions involving O_2. The most familiar one is dye-sensitized photooxidation involving transient singlet O_2 (Diels–Alder reaction of conjugated cyclic dienes, 'ene' reaction of olefins with allylic hydrogen, and dioxetane reaction of alkenes that do not feature an allylic H).[3] Another dye-sensitized photooxidation type involving molecular oxygen that is synthetically useful is sensitized electron-transfer oxygenation of hydrocarbons.[4] Especially attractive is the third reaction type, namely, hydrocarbon + O_2 photochemistry without the need of an added sensitizer. This involves photoexcitation of a hydrocarbon·O_2 charge-transfer state, and reactions so induced have been reported for small olefins (e.g. butenes) as well as larger systems (e.g. arylethenes) in solution,[5] at surfaces,[6] and in solid O_2.[7] However, in the case of small alkenes the corresponding absorption bands lie in the UV region. As a consequence, photolysis results in extensive fragmentation and/or rearrangement of the hydrocarbon skeleton and poor selectivity.

We have recently described in a preliminary report the discovery of a very strong, more than 10 000-cm^{-1} stabilization of the excited charge-transfer state of 2,3-dimethyl-2-butene·O_2 complexes inside the cages of zeolite NaY.[8] While the tail of the 2,3-dimethyl-2-butene (DMB)·O_2 charge-transfer absorption in the high-pressure O_2 gas and in O_2-saturated solution extends to 400 nm, we observed the onset of this absorption at 760 nm when loading the alkene and O_2 into zeolite NaY at −50 °C. The very substantial stabilization of the excited charge-transfer state is attributed to the electrostatic interactions inside the charged (but nonacidic) cages of NaY. Much less stabilization was observed when enclosing DMB and O_2 in the noncharged but still polar cages of high-silica faujasite. The charge-transfer absorption of DMB·O_2 in the zeolite matrix was detected by laser reaction excitation spectroscopy. The exclusive products of the long-wavelength light-induced DMB + O_2 reaction were 2,3-dimethyl-3-hydroperoxy-1-butene (> 90%) and acetone.

In this paper we will first present a full report of our study of the charge-transfer-induced DMB + O_2 photochemistry in zeolite NaY and in high-silica faujasite.[9] Then, a similar strong red shift of the *trans*- and *cis*-2-butene·O_2 charge-transfer absorption in zeolite NaY will be described. The long-wavelength light-

* Abstract published in *Advance ACS Abstracts*, February 15, 1994.

(1) Haber, J. In *Perspectives in Catalysis*; Thomas, J. M., Zamaraev, K. I., Eds.; IUPAC/Blackwell Scientific Publications: London, 1992; pp 371–385.

(2) (a) Parshall, G. W.; Ittel, S. D. *Homogeneous Catalysis*, 2nd ed.; Wiley: New York, 1992; pp 237–268. (b) Sheldon, R. A.; Kochi, J. K. *Metal-Catalyzed Oxidation of Organic Compounds*; Academic Press: New York, 1981.

(3) (a) *Singlet Oxygen*; Wasserman, H. H., Murray, R. W., Eds.; Academic Press: New York, 1979. (b) Matsumoto, M. In *Singlet O_2*; Frimer, A. A., Ed.; CRC Press: Boca Raton, FL, 1985; Vol. 2, Part 1, pp 205–272.

(4) (a) Foote, C. S.; Eriksen, J. *J. Am. Chem. Soc.* **1980**, *102*, 6083–6088. (b) Gilbert, A.; Baggott, J. *Essentials of Molecular Photochemistry*; Blackwell Scientific Publications: Oxford, U.K., 1991; pp 505–511. (c) Mattes, S. L.; Farid, S. In *Organic Photochemistry*; Padwa, A., Ed.; Dekker: New York, 1983; Vol. 6, pp 233–326. (d) Foote, C. S. *Tetrahedron* **1985**, *41*, 2221–2227.

(5) Onodera, K.; Furusawa, G.; Kojima, M.; Tsuchiya, M.; Aihara, S.; Akaba, R.; Sakuragi, H.; Tokumaru, K. *Tetrahedron* **1985**, *41*, 2215–2220.

(6) Aronovitch, C.; Mazur, Y. *J. Org. Chem.* **1985**, *50*, 149–150.

(7) (a) Hashimoto, S.; Akimoto, H. *J. Phys. Chem.* **1986**, *90*, 529–532. (b) *J. Phys. Chem.* **1987**, *91*, 1347–1354. (c) *J. Phys. Chem.* **1989**, *93*, 571–577.

(8) Blatter, F.; Frei, H. *J. Am. Chem. Soc.* **1993**, *115*, 7501–7502.

(9) For reviews on photochemistry in zeolites, see: (a) Turro, N. J. *Pure Appl. Chem.* **1986**, *58*, 1219–1229. (b) Ramamurthy, V. In *Photochemistry in Organized and Constrained Media*; Ramamurthy, V., Ed.; VCH Publishers: New York, 1991; pp 429–493. (c) Ramamurthy, V.; Eaton, D. F.; Caspar, J. V. *Acc. Chem. Res.* **1992**, *25*, 299–307. (d) Yoon, K. B. *Chem. Rev.* **1993**, *93*, 321–339.

0002-7863/94/1516-1812$04.50/0

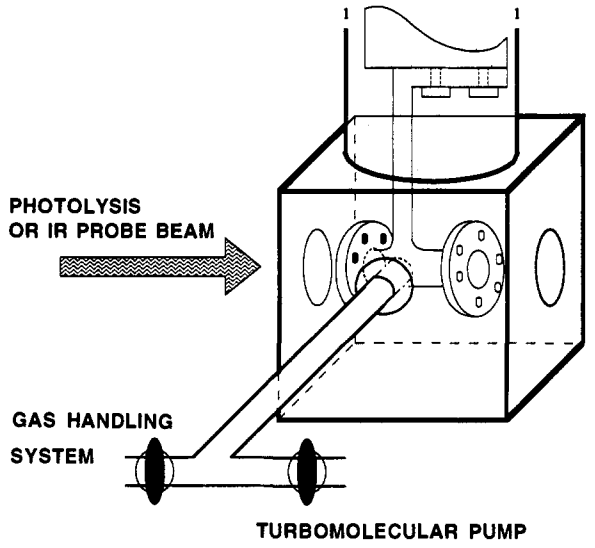

Figure 1. Scheme of the experimental setup.

induced reaction opened up by the strong stabilization of the charge-transfer state allowed us to synthesize for the first time 3-hydroperoxy-1-butene by direct excitation of 2-butene·O_2 pairs.

II. Experimental Section

Self-supporting zeolite wafers of approximately 10 mg (1.2-cm diameter) were prepared from powders of zeolite NaY (LZ-Y52, lot no. 03316X, Aldrich) or high-silica faujasite (prepared by treatment of zeolite NaY with $SiCl_4$,[10] Si/Al > 100 (IR analysis[11])) by aid of a KBr press. The pellets were placed inside a home-made miniature infrared vacuum cell (stainless steel) equipped with KBr windows. Vacuum-tight seals of the latter were achieved by using Viton O-rings for work in the temperature range between −50 °C and room temperature. Cooling of the IR cell below 220 K required the use of stainless steel spring-loaded Teflon O-rings (American Variseal Co., Part No. S62606-115-48S). The infrared cell was mounted inside an Oxford liquid nitrogen cryostat Model DN 1720 equipped with KBr windows. A schematic of the setup is shown in Figure 1. The temperature of the cryostat could be controlled within ±0.2 K over the range 77 K to 200 °C with an Oxford Instruments temperature controller Model TC-4. A feedthrough featuring a glass-to-metal transition furnished a vacuum connection between the IR cell inside the cryostat and the external gas handling and oil-free evacuation system (Varian turbomolecular pump Model V-60). A separate pumping system was used to maintain high vacuum in the Oxford cryostat.

Prior to loading with reactants, the zeolite pellet was dehydrated inside the IR cell by evacuation at 200 °C for 12–16 h. The state of dehydration was monitored by infrared spectroscopy. Subsequently, the temperature of the cell was adjusted to a value that allowed convenient loading of the alkene (typically −50 °C). After recording a background spectrum of the zeolite matrix, loading was accomplished by exposing the pellet to alkene gas well below its saturation pressure (500–700 mTorr in the case of 2,3-dimethyl-2-butene and 3,3-dimethyl-1-butene, 1–2 Torr in the case of *cis*- or *trans*-2-butene). Reactant pressure was monitored by an MKS Baratron Model 127A (range 10 mTorr to 10 Torr), and adsorption of the alkene was followed by IR spectroscopy. Typically 10 μmol of alkene was adsorbed on a 10-mg pellet. This corresponds to approximately 1.5 molecules per supercage, giving rise to a CH_3 bending mode absorption (around 1385 cm^{-1}) of 0.4 AU. Addition of 500 Torr of O_2 to the IR cell completed the loading procedure.

Photochemistry in the zeolite matrices was monitored by FT-infrared spectroscopy using an IBM-Bruker Model IR-97 spectrometer. For laser irradiation a prism-tuned Ar ion laser or an Ar ion laser pumped CW dye laser was used (Coherent Models Innova 90-6 and 599-01). The laser beam was expanded to the full size of the pellet. Laser emission in the region 540–780 nm was accomplished with the dyes Rhodamine 560, Rhodamine 590, DCM, and LDS 730 (all from Exciton). For photolysis with filtered tungsten source light, a water-cooled GE lamp Model Q250 was used in conjunction with Corning glass filters no. 3-72 ($\lambda \geq 430$ nm) and no. GG570 ($\lambda \geq 570$ nm). For light intensity measurements a Coherent power meter Model 210 was employed.

2,3-Dimethyl-2-butene (99%), 3,3-dimethyl-1-butene (95%, impurity 2,3-dimethyl-2-butene), 2,3-dimethyl-1-butene (97%, impurity mostly 2,3-dimethyl-2-butene), 3-buten-2-ol (98%), methyl vinyl ketone (99%), pinacolone (98%), and acetaldehyde (99%) were obtained from Aldrich Chemical Company. 3-Hydroxy-2,3-dimethyl-1-butene was obtained from Wiley Organics (98%), and *trans*-2-butene (99%) and *cis*-2-butene (95%) from Matheson. *trans*- and *cis*-2,3-epoxybutane were obtained from Aldrich (97%). All these chemicals were distilled in a vacuum line before use. N_2O (99%) and O_2 (99.997%) were obtained from Matheson, and $^{18}O_2$ (98 atom % D) was obtained from Cambridge Isotope Laboratories and used as received.

III. Results

We will first present infrared spectral data that allowed us to identify the products of the photoinduced alkene + O_2 reactions in zeolites NaY and high-silica faujasite (HSF) (section 1). In section 2, laser reaction excitation spectra will be presented which reveal the reactant electronic absorption responsible for the observed chemistry. The thermal reaction that occurred in the case of 2,3-dimethyl-2-butene (DMB) + O_2 in the room temperature zeolite will be discussed in section 3.

1. Identification of Photochemical Products. 1.1. 2,3-Dimethyl-2-butene + O_2. a. NaY. The infrared difference spectrum taken upon loading of DMB into zeolite NaY at −50 °C revealed reactant absorptions of molecules inside the zeolite at 1385, 1400, 1464, 1657, 2740, 2870, 2920, and 2990 cm^{-1}. Infrared absorptions of molecules inside the zeolite can readily be measured in the range 4000–1250 cm^{-1}, while the region below 1250 cm^{-1} is partly opaque due to intense Si–O (Al–O) lattice vibrations. Nevertheless, spectra in the regions 930–800 and 750–650 cm^{-1} can be obtained with reduced sensitivity. The region between 1800 and 800 cm^{-1} of DMB-loaded zeolite NaY is shown in Figure 2a. No new bands appeared upon subsequent loading of the zeolite by O_2 or when leaving the DMB- and O_2-containing matrix at −50 °C in the dark for prolonged periods (up to 14 h).

Irradiation of the loaded NaY zeolite with light at wavelengths shorter than 760 nm resulted in the decrease of all DMB bands and concurrent growth of the product absorptions displayed in Table 1. Corresponding photolysis experiments with $^{18}O_2$-loaded NaY furnished the ^{18}O product frequency shifts shown in the second column of the table. An infrared difference spectrum obtained upon 30-min photolysis with 514-nm light (400 mW cm^{-2}) is shown in Figure 2b (a spectrum following irradiation with red light has been presented in Figure 1 of the preceding communication).[8] No reaction was observed upon irradiation at these wavelengths, power levels, and exposure times if the zeolite matrix contained only alkene, or only O_2.

All the infrared product bands of Table 1, with the exception of the feature at 1708 cm^{-1}, originate from 2,3-dimethyl-3-hydroperoxy-1-butene. This was established by recording a spectrum of an authentic sample of the latter upon loading into an NaY matrix, as shown in Figure 3. The hydroperoxide was synthesized by the singlet O_2 method described by Schenck.[12] The assignment was further supported by the observation of small but significant ^{18}O isotope frequency shifts. The 1708-cm^{-1} product band coincides with the ν(C=O) absorption of a $CH_3C(=O)CH_3$ sample in NaY. The observed ^{18}O shift of 28 cm^{-1} of this band corroborates this assignment. Since the growth of this most intense band of acetone is small, it can readily be understood why no other infrared absorption of this product is observed. We conclude that 2,3-dimethyl-3-hydroperoxy-1-

(10) (a) Beyer, H. K.; Belenykaja, I. M.; Hauge, F.; Tielen, M.; Grobet, P. J.; Jacobs, P. A. *J. Chem. Soc., Faraday Trans. 1* **1985**, *81*, 2889–3006. (b) Blatter, F.; Schumacher, E. *J. Chem. Educ.* **1990**, *67*, 519–526.

(11) Anderson, M. W.; Klinowski, J. *J. Chem. Soc., Faraday Trans. 1* **1986**, *82*, 1449–1469.

(12) Schenck, G. O.; Schulte-Elte, K. H. *Justus Liebigs Ann. Chem.* **1958**, *618*, 185–193.

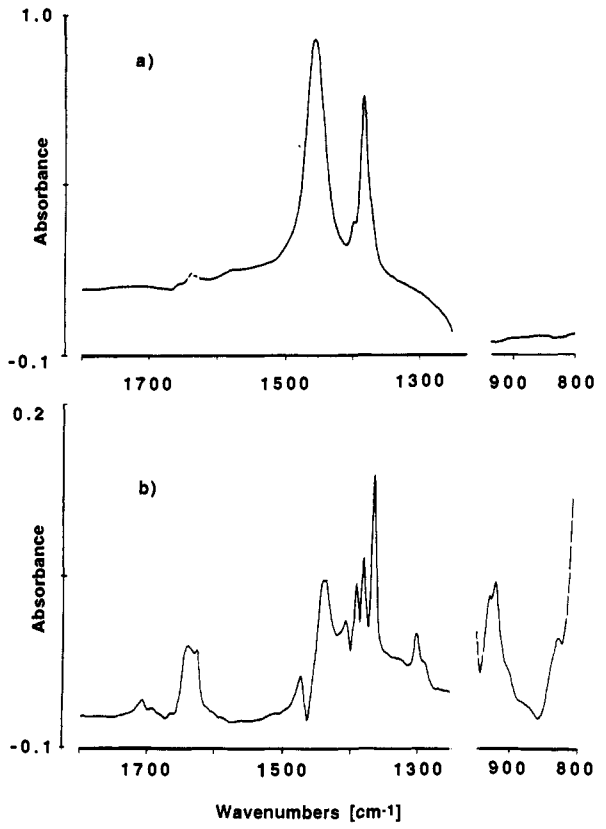

Figure 2. (a) Infrared difference spectrum before and after adsorption of 2,3-dimethyl-2-butene on zeolite NaY at 223 K in the presence of 500 Torr of O_2. (b) Infrared difference spectrum before and after Ar ion laser photolysis at 514 nm (30 min, 400 mW cm^{-2}). The dashed lines indicate opaque regions due to strong zeolite absorption bands.

Table 1. Infrared Product Spectra of DMB + O_2 Assigned to 2,3-Dimethyl-3-hydroperoxy-1-butene (DHB) and Acetone (A)

frequency, cm^{-1}				
NaY		HSF		
DMB + O_2	DMB + $^{18}O_2$[a]	DMB + O_2	DMB + $^{18}O_2$[a]	assignment
830				$\gamma_{o.p.}(CH_2)$, $\nu(OO)$, $\nu(CC)$, $\gamma(CH_3)$, DHB
875				
905				
920		925		
1302		1302		$\nu(CC)$, $\gamma_{i.p.}(CH_2)$, DHB
1365		1368		$\delta_s(CH_3)$, DHB, A
1384[b]	-1			$\delta_s(CH_3)$, DHB
1407[b]	-2			
		1420		$\delta_a(CH_3)$, A
1440[b]				
1460[b]		1470		$\delta_a(CH_3)$, DHB
		1480		
1628		1634		$\nu(C{=}C)$, DHB
1641				
1708	-28	1711[c]	-37[d]	$\nu(C{=}O)$, A
2850				$\nu_s(CH_3)$, DHB
2960		2946		$\nu_a(CH_3)$, DHB, A
2990		2980		$\nu_a(CH_3)$, DHB, A
3080				$\nu(CH_2)$, DHB
3200[e]	≈-10	3350[f]	≈-10	$\nu(OH)$, DHB

[a] Frequency shift upon ^{18}O substitution. The perturbed baseline did not allow us to determine isotope frequency shifts for product bands below 1000 cm^{-1}. [b] Product band overlapped by decreasing DMB absorption. [c] Shoulder at 1680 cm^{-1}. [d] Isotope shift measurement rendered difficult by band-shape change upon ^{18}O substitution. [e] Very broad, fwhm ≈ 250 cm^{-1}. [f] Very broad, fwhm ≈ 400 cm^{-1}.

butene (major, >90%) and acetone (minor) are the only products of visible or near-infrared light-induced DMB + O_2 chemistry in zeolite NaY.

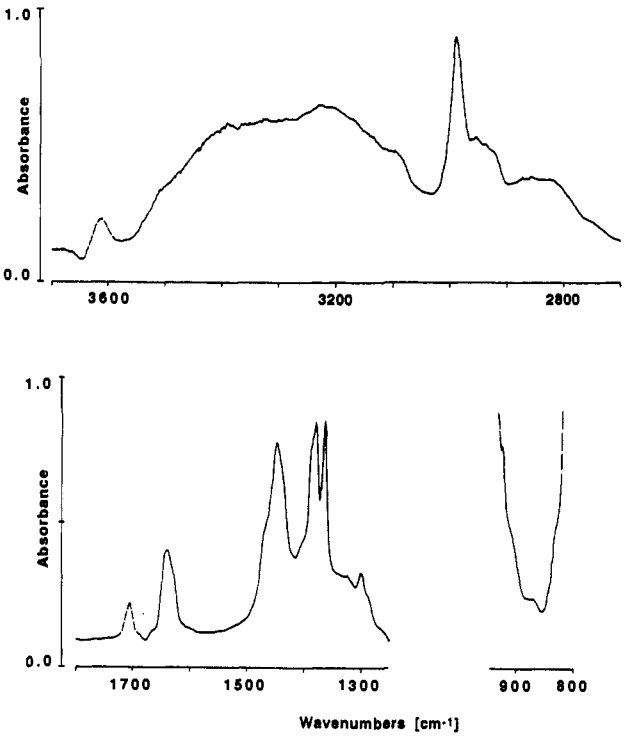

Figure 3. Authentic spectrum of 2,3-dimethyl-3-hydroperoxy-1-butene adsorbed on zeolite NaY at 223 K. Loading was conducted at 273 K. The ν(OH) peak at 3610 cm^{-1} does not exhibit any ^{18}O frequency shift and, hence, is attributed to an impurity. The small peak at 1708 cm^{-1} is due to acetone impurity in the hydroperoxide sample.

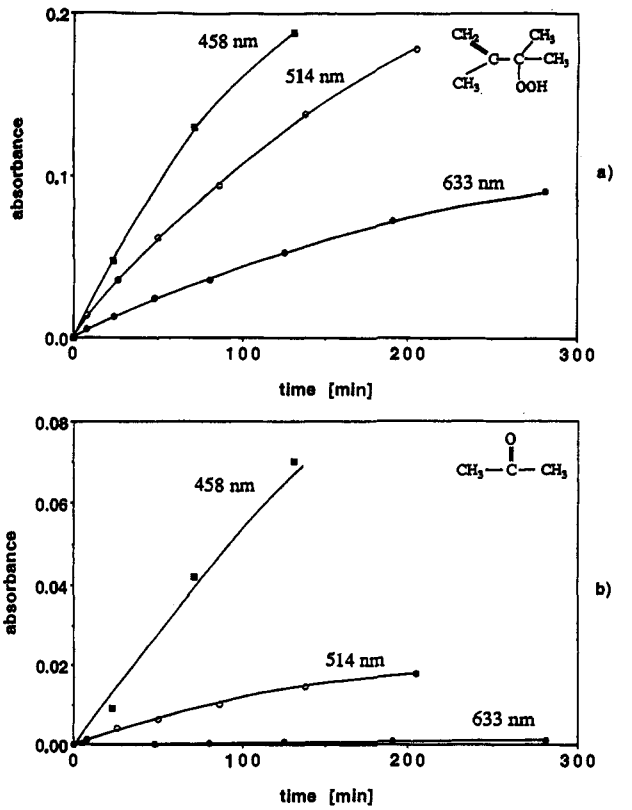

Figure 4. Absorbance growth kinetics for two different IR absorption bands (a) at 1365 cm^{-1} (hydroperoxide) and (b) at 1708 cm^{-1} (acetone) at three different photolysis wavelengths: 633, 514, and 458 nm.

The kinetics of absorbance growth of both products at 633, 514, and 458 nm is shown in Figure 4. No induction period or sigmoidal behavior is observed at any wavelength. This is consistent with both products emerging from single-photon DMB

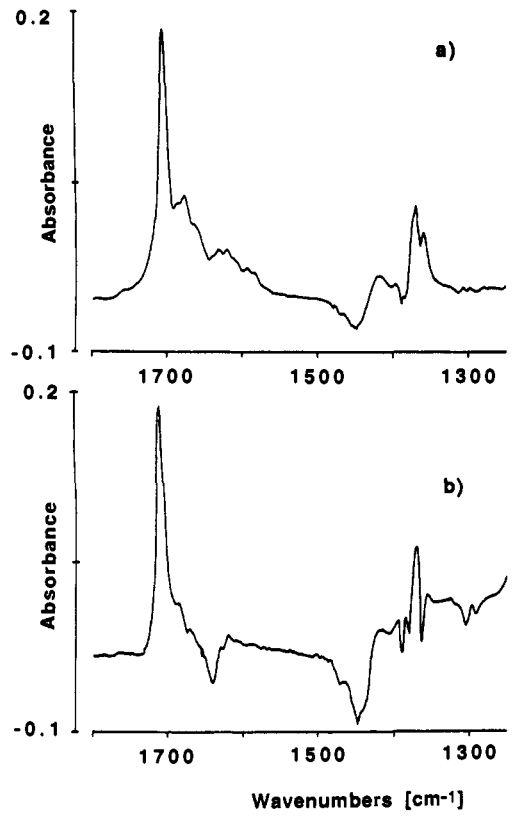

Figure 5. (a) Infrared difference spectrum before and after warm-up of the DMB/O_2/NaY matrix (from −50 °C to 20 °C) after build-up of 2,3-dimethyl-3-hydroperoxy-1-butene produced by photolysis with visible light. (b) Infrared difference spectrum showing the decomposition of synthesized 2,3-dimethyl-3-hydroperoxy-1-butene after adsorption on NaY and warm-up of the zeolite matrix from −50 °C to room temperature.

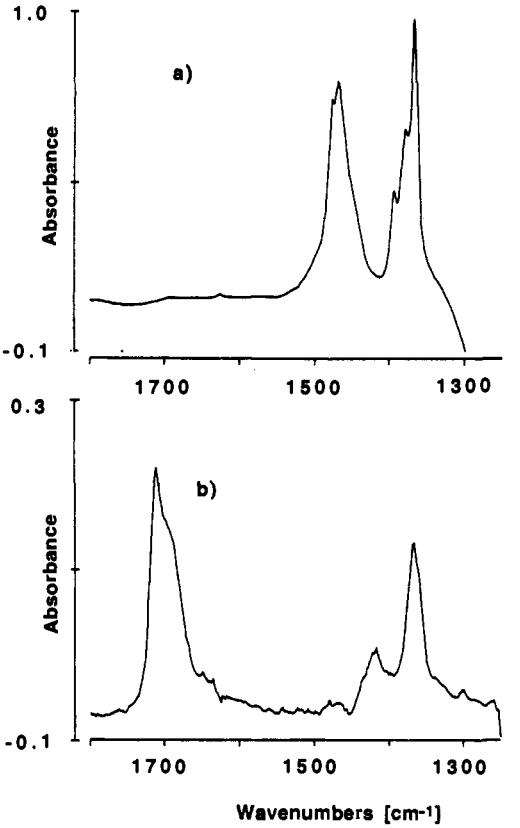

Figure 6. (a) Infrared difference spectrum before and after loading of high-silica faujasite with 2,3-dimethyl-2-butene and O_2 at −50 °C. The small band at 1628 cm^{-1} originates from an impurity. (b) Infrared difference spectrum before and after photolysis with CW Ar ion laser light at 514 nm for 60 min at 400 mW cm^{-2}.

+ O_2 photochemistry and shows that no secondary photolysis occurs. Furthermore, comparison of the wavelength dependence of the growth curves shows that the branching ratio acetone/hydroperoxide increases toward higher photon energies. Determination of the relative extinction coefficients of the acetone and hydroperoxide infrared bands in the thermal decomposition experiments (see below) revealed that upon 633-nm photolysis the acetone/hydroperoxide branching ratio is less than 0.01.

Using unfiltered light from a tungsten source, the same product growth was obtained (within 5%) as in a 514-nm laser photolysis experiment at equal light intensity and exposure time. Similarly, filtered tungsten lamp irradiation at $\lambda > 570$ nm gave very similar product spectra as obtained upon 633-nm laser irradiation. In particular, the change of the acetone/hydroperoxide branching ratio when increasing the photolysis wavelength was reproduced in the tungsten lamp experiments. This demonstrates that the alkene + O_2 photochemistry can readily be achieved with the emission of a conventional broad-band lamp. The special advantage of using tuned CW laser light in this work is the elucidation of the wavelength dependence of the photochemistry.

At the zeolite temperature at which the DMB + O_2 photoreactions were conducted, namely −50 °C, the hydroperoxide product was found to be stable in zeolite NaY. Warm-up of the matrix to room temperature resulted in slow thermal decomposition of the latter to acetone (half-life of about 24 h at O °C). Figure 5a shows the infrared difference spectrum upon warm-up to 20 °C (rate: 1 degree per min) of a DMB- and O_2-loaded NaY matrix that had been irradiated with visible light for a prolonged period. The only product that can clearly be identified is acetone (1708 cm^{-1} (^{18}O shift of 28 cm^{-1}) and 1370 cm^{-1}). The same thermal chemistry was observed upon decomposition of an authentic sample of the hydroperoxide in NaY (Figure 5b). Acetone is the main decomposition product of 2,3-dimethyl-3-hydroperoxy-1-butene in slightly acidic solution.[12]

b. High-Silica Faujasite. Adsorption of DMB on high-silica faujasite yielded the infrared spectrum shown in Figure 6a. Alkene bands are at 1366, 1380, 1394, 1468, 1477, 1660, 2871, and 2970 cm^{-1}. As in the case of experiments in NaY, no new absorptions appeared upon subsequent exposure of the DMB loaded HSF to 500 Torr of O_2 gas or when keeping the DMB/O_2/HSF matrix for prolonged times in the dark at −50 °C. Spectral changes upon irradiation of the sample at 514 nm (400 mW cm^{-2} for 1 h) are shown in Figure 6b, and the product bands, including ^{18}O frequency shifts, are presented in Table 1. The longest wavelength at which reaction could be induced was 600 nm. Comparison with spectra of authentic samples of acetone and 2,3-dimethyl-3-hydroperoxy-1-butene shows that all product bands are accounted for by these two species. However, the branching ratio acetone/hydroperoxide is shifted strongly in favor of acetone compared to the distribution in NaY. This can readily be seen from a comparison of Figures 6b and 2b.

2,3-Dimethyl-3-hydroperoxy-1-butene loaded into zeolite NaY is indefinitely stable at −50 °C, but the species decomposes slowly inside HSF even at this temperature. Therefore, part of the acetone must emerge from decomposing hydroperoxide as it accumulates upon DMB + O_2 photolysis. However, we found that the branching ratio acetone/hydroperoxide is substantially larger than in NaY even when conducting DMB + O_2 photochemistry in HSF zeolite cooled to 110 K. At this temperature, no thermal decomposition of the hydroperoxide occurs. Hence, we conclude that the acetone/hydroperoxide branching upon photoexcitation of DMB·O_2 shifts in favor of acetone when NaY is replaced by high-silica faujasite.

1.2. trans- and cis-2-Butene + O_2. Zeolite NaY loaded with *trans*-2-butene showed infrared absorptions at 1300, 1386, 1440,

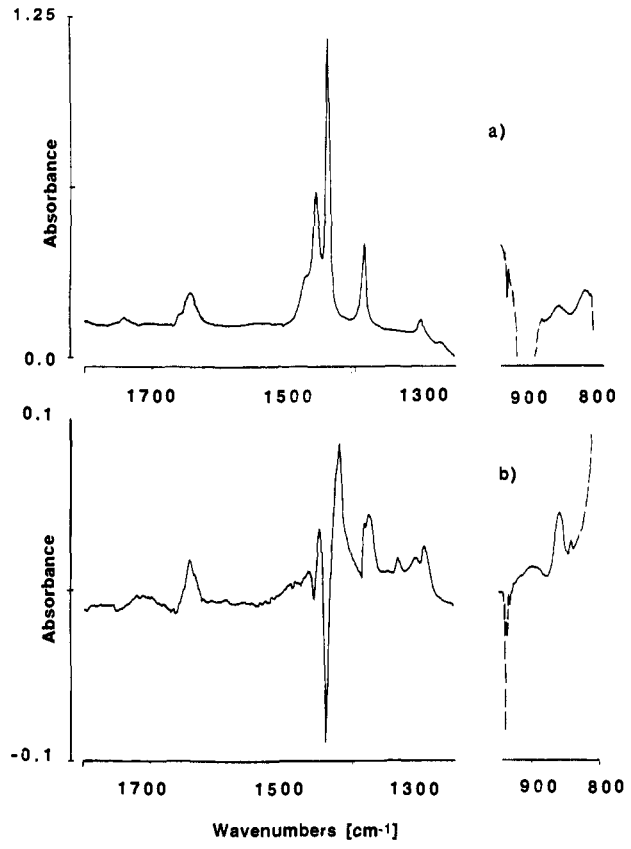

Figure 7. (a) Infrared difference spectrum before and after loading of zeolite NaY with *trans*-2-butene and O_2 at −50 °C. (b) Infrared difference spectrum before and after photolysis with CW Ar ion laser light at 514 nm (30 min, 400 mW cm^{-2}) at 223 K. Dashed lines indicate opaque regions due to the strong zeolite absorptions.

1458, 1474, 1660, 2750, 2892, 2923, 2948, 2966, and 3010 cm^{-1}. The spectrum in the region below 1800 cm^{-1} is shown in Figure 7a. No evidence of thermal chemistry was noticed upon subsequent loading of the zeolite with O_2 or when keeping *trans*-2-butene- and O_2-loaded NaY for prolonged periods in the dark at room temperature. Also, no absorption changes occurred when irradiating an NaY matrix that contained only the alkene with visible laser light.

Irradiation of *trans*-2-butene- and O_2-containing zeolite NaY with light at wavelengths shorter than 600 nm resulted in loss of alkene absorption and concurrent growth of the infrared bands listed in Table 2. The ^{18}O isotope frequency shifts are also presented in the table. An infrared difference spectrum showing the effect of 30-min irradiation at 514 nm (400 mW cm^{-2}) is shown in Figure 7b.

Observation of bands at 3150 (^{18}O shift of 10 cm^{-1}), 1640, and 857 cm^{-1} signals ν(OH), ν(C=C), and $\gamma_{o.p.}$ (CH_2, vinyl) modes, respectively.[13] This is consistent with the structure CH_2=CH—CH(CH_3)—OOH, the product expected on the basis of the result of the DMB + O_2 photochemistry in NaY. Assignment of the 857-cm^{-1} band to the out-of-plane CH_2 wagging mode of the vinyl group presupposes a shift of 50 cm^{-1} to lower frequencies relative to the position of the corresponding gas-phase band.[13] Indeed, we have observed a similar red shift of $\gamma_{o.p.}$ (CH_2, vinyl) of 32 cm^{-1} when loading (CH_3)$_3$C—CH=CH_2 into zeolite NaY. The empirical vibrational assignments for the remaining product bands are given in Table 2. Frequencies agree well with literature values for the corresponding group modes.[13] Hence, the vibrational data suggest that the photochemical reaction of *trans*-2-butene with O_2 in zeolite NaY gives CH_2=CH—CH(CH_3)—OOH. This conclusion is supported by the thermal decomposition

(13) Colthup, N. B.; Daly, L. H.; Wiberley, S. E. *Introduction to Infrared and Raman Spectroscopy*, 3rd ed.; Academic Press: New York, 1990.

Table 2. Infrared Product Spectra of *trans*- or *cis*-2-Butene + O_2 Assigned to 3-Hydroperoxy-1-butene[a]

frequency, cm^{-1} NaY		
t-butene + O_2	*t*-butene + $^{18}O_2$[b]	assignment
844		ν(OO)[c]
857		$\gamma_{o.p.}$(CH_2)
1294	−2	γ(CH, vinyl)
1305		ν(CC)
1335		δ(CH, tertiary)
1375		
1386		δ_s(CH_3)
1419		δ(CH_2)
1428	−1	
1455	−2	δ_a(CH_3)
1640		ν(C=C)
2825		
2848		ν_s(CH_3)
2903		ν(CH, tertiary)
2983		ν_a(CH_3), ν_s(CH_2)
		ν(CH, vinyl)
3089		ν_a(CH_2)
3150[d]	≈−10	ν(OH)

[a] In some photolysis experiments a small absorption was observed at 1720 cm^{-1} (^{18}O shift 27 cm^{-1}), which may be due to acetaldehyde. The growth of this band was not reproducible. [b] Frequency shift upon ^{18}O substitution. The perturbed baseline did not allow us to determine isotope shifts for product bands below 1000 cm^{-1}. [c] Tentative, since a low S/N did not permit observation of the ^{18}O counterpart. [d] Very broad, fwhm ≈ 250 cm^{-1}.

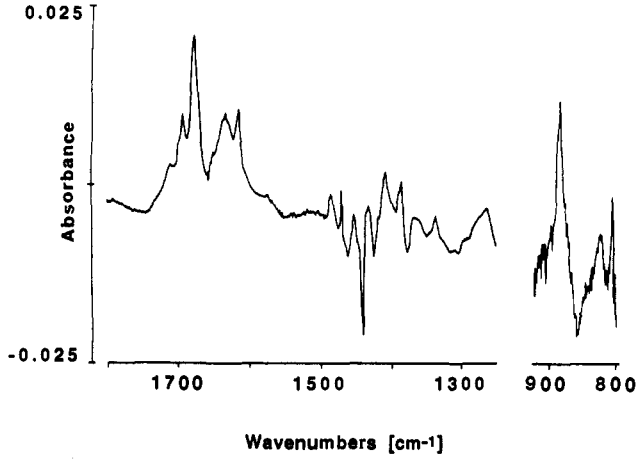

Figure 8. Infrared difference spectrum before and after warm up from −50 °C to 0 °C of the photolysed *trans*-2-butene/O_2/NaY matrix. Positive bands originate from thermal decomposition of the photolysis product. The absorbance scale of the 900–800 cm^{-1} region is expanded by a factor of 2.

products observed upon warm-up of the zeolite. Figure 8 shows the infrared difference spectrum obtained upon increase of the temperature from −50 to 0 °C of a matrix in which *trans*-2-butene + O_2 photoproduct has been accumulated by prolonged 514-nm irradiation. Bands at 1265 (s-trans), 1280 (s-cis), 1409, 1616, 1636, 1679 (s-trans), 1695 (s-cis), and 2930 cm^{-1} coincide with those of CH_2=CH—C(=O)—CH_3 in NaY (s-trans and s-cis conformers were both formed). Additional absorptions at 827, 1265, 1336, 1386, 1636, 2880, and 2975 and a very broad feature around 3450 cm^{-1} (fwhm ≈ 250 cm^{-1}) agree well with the spectrum of CH_2=CH—CH(CH_3)—OH in zeolite NaY. Infrared spectra of authentic samples of these two species were recorded under the same conditions as used in the *trans*-2-butene + O_2 experiments. Assignment of s-trans and s-cis conformer bands of methyl vinyl ketone was based on UV-light-induced perturbation of the conformer population in NaY using an Nd:YAG laser as photolysis source (355 nm). Three product bands of the thermolysis spectrum (Figure 8) that remain to be identified

are at 812, 887, and 1486 cm^{-1}. They coincide with those of an authentic *trans*-2,3-epoxybutane sample in zeolite NaY (however, these bands do not agree with the spectrum of the cis diastereomer). We attribute *trans*-2,3-epoxybutane and 3-hydroxy-1-butene products to the thermal reaction of 3-hydroperoxy-1-butene with excess *trans*-2-butene. This conclusion is based on a separate experimental observation in the case of the *cis*-2-butene + O_2 photochemistry described below. By contrast, methyl vinyl ketone (and H_2O) emerges from thermal rearrangement of the photochemical product 3-hydroperoxy-1-butene. CH_2=CH—C(=O)—CH_3 is also known to be the thermal decomposition product of 3-hydroperoxy-1-butene in butanol or acetic acid solution.[14,15] Hence, all products observed upon warm-up of the photolysed NaY matrix support our initial conclusion that the sole product of the photochemical *trans*-2-butene + O_2 reaction in the zeolite is 3-hydroperoxy-1-butene.

We have conducted an identical photochemical study of the *cis*-2-butene + O_2 reaction in zeolite NaY. *cis*-2-Butene has infrared absorptions at 870, 1363, 1389, 1409, 1444, 1461, 1647, 2758, 2868, 2927, 2951, 2979, and 3008 cm^{-1}. Irradiation at 514 nm gave product spectra and yields identical with those of the *trans*-2-butene + O_2 system. No photo-interconversion to the more stable *trans*-2-butene was detected. Thermal reaction upon warm-up of an irradiated *cis*-2-butene/O_2/NaY matrix (in which 3-hydroperoxy-1-butene had been accumulated) yielded methyl vinyl ketone, 3-hydroxy-1-butene, and growth at 887, 1280, 1399, and 1483 cm^{-1}. These four bands coincide with those of an authentic spectrum of *cis*-2,3-epoxybutane in NaY. No *trans*-epoxybutane could be detected. Signal-to-noise levels allowed us to conclude that the *cis*/*trans*-epoxide branching ratio has a lower limit of 15. We attribute the epoxide and the alcohol products to the thermal reaction of 3-hydroperoxy-1-butene with the 2-butene. This assignment was established by the observation that only methyl vinyl ketone, but no epoxide or alcohol, was produced when removing the 2-butene by evacuation prior to warm-up of the hydroperoxybutene-loaded matrix.

Attempts were made to observe reaction upon photoexcitation of *trans*-2-butene and O_2 in high-silica faujasite. Product growth was observed upon irradiation at 514 nm and shorter wavelengths. However, even at these short wavelengths the absorbance growth was too slow to permit product identification by infrared analysis.

1.3. 3,3-Dimethyl-1-butene + O_2. Similar visible-light-induced chemistry was attempted for NaY matrices loaded with O_2 and 3,3-dimethyl-1-butene. No reaction was observed at any visible wavelength, not even upon prolonged Ar ion laser irradiation at 458 nm.

2. Laser Reaction Excitation Spectra. When the infrared product absorbance growth of the DMB + O_2 reaction in NaY was monitored for a fixed number of photolysis photons and the laser was tuned from 760 to 476 nm, the reaction excitation spectrum of Figure 9 was obtained. Each data point of this curve represents the absorbance growth of the 1365-cm^{-1} $\delta_s(CH_3)$ absorption of 2,3-dimethyl-3-hydroperoxy-1-butene upon irradiation with 2.8 × 10^{21} photons (corresponding, at 760 nm, to 30-min photolysis at 400 mW cm^{-2}). This profile reflects the product of the reactant extinction coefficient and the reaction quantum efficiency. Diffuse reflectance spectra taken in our laboratory of NaY loaded with DMB alone (or other small alkenes like ethylene, propene, 2-butene, 2-methyl-2-butene) do not exhibit any absorption between 250 and 800 nm.[16] This confirms that adsorption of alkene on inert zeolite NaY does not give rise to

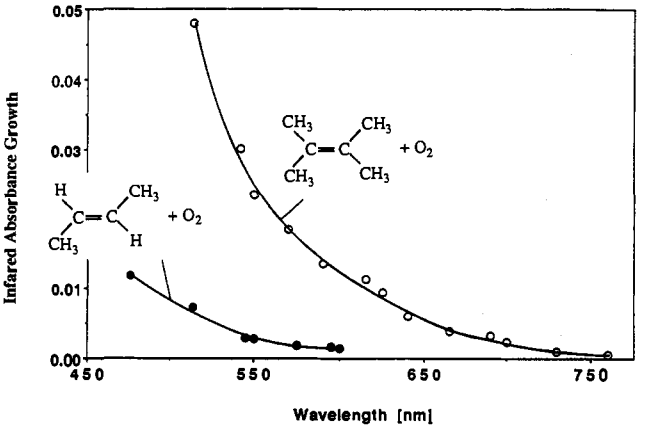

Figure 9. Laser reaction excitation spectra of 2,3-dimethyl-2-butene/O_2 and *trans*-2-butene/O_2 in zeolite NaY. Each point of the curves represents the absorbance growth of the hydroperoxide photoproduct absorption at 1365 cm^{-1} (2,3-dimethyl-3-hydroperoxy-1-butene) and 1378 cm^{-1} (3-hydroperoxy-1-butene) upon irradiation with 3 × 10^{21} photons.

an alkene·zeolite lattice electronic transition in this region.[8,17,18] Likewise, no diffuse reflectance spectrum is observed when exposing the zeolite to 500 Torr of O_2. However, simultaneous loading of NaY with DMB (or other butenes) and O_2 results in a continuous absorption band in the UV and visible regions which could be reversibly removed by pumping away the oxygen. This work will be reported in a forthcoming paper.[16] Figure 9 also depicts a laser reaction excitation spectrum for *trans*-2-butene + O_2 in zeolite NaY. Each point of the curve gives the absorbance growth of the 1375-cm^{-1} $\delta_s(CH_3)$ absorption of 3-hydroperoxy-1-butene upon irradiation with 3.5 × 10^{21} photons. Concentrations of O_2 and alkene in the zeolite were chosen to be the same as those in the DMB + O_2 case. This was accomplished by adjusting the *trans*-2-butene concentration so as to obtain the same intensity for the $\delta_s(CH_3)$ absorption of the two alkenes.

3. Thermal DMB + O_2 Reaction. When DMB- and O_2-loaded NaY or HSF was warmed above temperatures of −20 °C, a dark thermal reaction was observed. By contrast, no thermal chemistry occurred in the case of *trans*- (or *cis*-) 2-butene and O_2-loaded zeolite even at room temperature. We have studied the dark DMB + O_2 reaction in zeolite NaY by loading the matrix with DMB and O_2 at −50 °C and then monitoring the spectral changes upon warm-up of the pellet at a rate of 1 deg min^{-1} by FT-infrared spectroscopy. An infrared difference spectrum taken upon warm-up of DMB/O_2/NaY to 0 °C showed loss of DMB absorption under concurrent infrared product growth at 1241, 1284 (−2), 1327 (−1), 1365, 1384, 1396, 1437, 1450, 1468, 1482 (−2), 1628, 1670 (−27), 1700 (−29), 2966, and 3400 cm^{-1} (very broad), as shown in Figure 10a. Numbers in parentheses indicate ^{18}O frequency shifts observed when conducting the reaction with $^{18}O_2$. Comparison with the infrared spectrum of an authentic sample of pinacolone (3,3-dimethyl-2-butanone), displayed in Figure 10b, indicates that this ketone is a main product of the thermal DMB + O_2 reaction in zeolite NaY. This leaves weak product bands at 1241, 1384, 1437, and 1450 cm^{-1}, and moderately strong features at 1628, 1670, and 3400 cm^{-1} yet to be assigned.[19] The bands at 1670 (^{18}O shift 27 cm^{-1}) and 1628 cm^{-1} are characteristic of ν(C=O) and ν(C=C), respectively, of an α,β-unsaturated ketone.[13] The most likely candidate is CH_2=C(CH_3)—C(=O)—CH_3, which would be

(14) Chernyak, B. I.; Koshovskii, B. I.; Borovaya, V. G. *Zh. Org. Khim.* **1971**, *7*, 625–628.
(15) Frimer, A. A.; Stephenson, L. M. In ref 3b, p 67.
(16) Blatter, F.; Moreau, F.; Frei, H. To be submitted.
(17) Zeolite NaY dehydrated at temperatures below 400 °C does not exhibit any Lewis acid sites that could give rise to alkene·lattice charge-transfer transitions.[18]
(18) Ward, J. W. *J. Catal.* **1968**, *10*, 34–46.
(19) One additional band at 1610 cm^{-1} (at 1590 cm^{-1} in the $^{18}O_2$ experiment) exhibited intensities which varied strongly from experiment to experiment. No assignment can be given at this point.

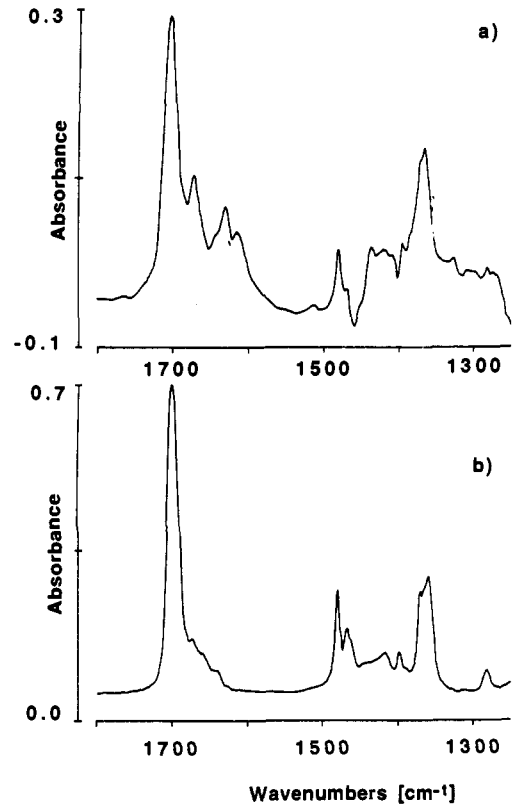

Figure 10. (a) Infrared difference spectrum before and after thermal 2,3-dimethyl-2-butene + O_2 reaction in zeolite NaY at O °C for 14 h. (b) Infrared difference spectrum before and after adsorption of 3,3-dimethyl-2-butanone (pinacolone) on zeolite NaY at a concentration of approximately one molecule per supercage.

coproduced with CH_3OH. No authentic sample of the enone was available for recording of spectra in NaY. An authentic spectrum of methanol in the zeolite showed that all its bands, except the very broad O–H stretch at 3400 cm^{-1}, would overlap with reactant or other product absorptions. Hence, assignment of the enone and methanol products remains tentative at this point. It is interesting to note that 2,3-dimethyl-3-hydroperoxy-1-butene (major) and acetone (minor) are the sole products of the photochemical DMB + O_2 reaction even at room temperature. These can easily be monitored independently of the thermal DMB + O_2 reaction because the photochemical reaction rate at 514 nm and 400 mW cm^{-2} laser power is high compared to the thermal oxidation rate at this temperature.

IV. Discussion

We will first discuss the assignment of the long-wavelength electronic absorption of alkene·O_2 responsible for the observed chemistry. Then, a mechanism for the photochemical alkene + O_2 reaction will be proposed, followed by a brief discussion of the thermal DMB + O_2 reaction path in the room temperature NaY matrix.

1. Assignment of Electronic Transition. Faujasite-type zeolites, like NaY and high-silica faujasite (HSF) used here, feature a three-dimensional network of supercages. These spherical cages have a diameter of about 13 Å and are interconnected by windows with 8-Å openings.[20] The principal difference between zeolites NaY and HSF lies in the electrostatic environment of the cages. NaY contains univalent cations in the supercage and in other, smaller internal spaces of the zeolite (sodalite cage, hexagonal cage)[20] while HSF does not. The charges of the Na^+ ions in NaY compensate the negative charge on the oxygens of the cage walls that originates from the presence of Al in the framework (NaY: Si/Al ≈ 2.5, seven Na^+ per supercage). By contrast, the majority of the cages of HSF contain no free charge (Si/Al > 100), although infrared spectra reveal some remaining silanol groups.

We can conceive of two possibilities for the appearance of a visible (near-infrared) electronic transition upon coadsorption of DMB or 2-butene and O_2 on the zeolite. One is an O_2-enhanced triplet absorption of the alkene, the other an alkene·O_2 charge-transfer absorption. The first-mentioned possibility can be ruled out because the lowest triplet states of small alkenes in conventional environments (gas, liquid, solid) lie in the UV region.[21] Phosphorescence studies, e.g. as reported by Ramamurthy,[9b,c] have shown that spectral shifts of triplet states upon loading of simple organics into zeolites are small. By contrast, assignment to an alkene·O_2 charge-transfer transition is strongly supported by the observed dependence of the photochemical reaction threshold on the ionization potential of the hydrocarbon.[22] Among the olefins we studied, DMB has the lowest ionization potential, namely 8.30 eV,[23] and exhibits the lowest reaction threshold energy with O_2 (760 nm, corresponding to 1.63 eV). *trans*-2-Butene + O_2 has its reaction threshold at a substantially shorter wavelength, 600 nm (corresponding to 2.07 eV). This reflects the higher ionization potential of CH_3—CH=CH—CH_3 (9.13 eV) compared to DMB.[23] 3,3-Dimethyl-1-butene does not react even upon excitation at 458 nm (corresponding to 2.71 eV). This is consistent with the high ionization potential of 9.51 eV of this hydrocarbon. Hence, the onset of the reaction excitation spectrum shifts monotonically to higher energies with increasing ionization potential of the alkene, as expected for a charge-transfer transition. However, in a plot of the reaction threshold energy versus alkene ionization potential, the data points for DMB, 2-butene, and 3,3-dimethyl-1-butene do not lie on a straight line. This has its origin most probably in reaction quantum efficiency differences for the three systems (see subsection 2 below).

An intriguing implication of this assignment is the very large red shift of about 300 nm relative to charge-transfer absorptions in conventional environments. Alkene·O_2 contact charge-transfer absorptions have been reported in oxygen-saturated organic solution,[5,24] high-pressure O_2 gas,[25] and a solid O_2 matrix.[7,26] Red shifts of hydrocarbon·O_2 charge-transfer absorptions from gas phase to solution[27] or to solid O_2[7,26] are small (at most 10 nm).[28] Similarly, changing the polarity of the organic solvent over a wide range has little effect on the alkene·O_2 charge-transfer absorption.[24] The onset of the *cis*- or *trans*-2-butene·O_2 charge-transfer absorption in any of the three phases (gas, solution, solid O_2) is around 350 nm.[7b,25] Our observation of a reaction threshold at 600 nm in zeolite NaY implies a 12 000-cm^{-1} stabilization of

(20) (a) Breck, D. W. *Zeolite Molecular Sieves: Structure, Chemistry, and Use*; Wiley: New York, 1974. (b) Bhatia, S. *Zeolite Catalysis: Principles and Applications*; CRC Press, Inc.: Boca Raton, FL, 1989; p 12. (c) *Introduction to Zeolite Science and Practice, Studies in Surface Science and Catalysis*; van Bekkum, H., Flanigen, E. M., Jansen, J. C., Eds.; Elsevier: Amsterdam, The Netherlands, 1991; Vol. 58.

(21) Murov, S. L. *Handbook of Photochemistry*; Marcel Dekker: New York, 1973.

(22) Birks, J. B. *Photophysics of Aromatic Molecules*; Wiley: London, 1970; p 406.

(23) *CRC Handbook of Chemistry and Physics*, 53rd ed.; Weast, R. C., Ed.; The Chemical Rubber Co.: Cleveland, OH, 1972; p E-62.

(24) (a) Evans, D. F. *J. Chem. Soc.* **1953**, 345–347. (b) Tsubomura, H.; Mulliken, R.S. *J. Am. Chem. Soc.* **1960**, *82*, 5966–5974. (c) Coomber, J. W.; Hebert, D.M.; Kummer, W. A.; Marsh, D. G.; Pitts, J. N., Jr. *Environ. Sci. Technol.* **1970**, *4*, 1141–1145.

(25) Itoh, M.; Mulliken, R. S. *J. Phys. Chem.* **1969**, *73*, 4332–4334.

(26) Rest, A. J.; Salisbury, K.; Sodeau, J. R. *J. Chem. Soc., Faraday Trans. 2* **1977**, *73*, 265–273.

(27) (a) Lim, E. C.; Kowalski, V. L. *J. Chem. Phys.* **1962**, *36*, 1729–1732. (b) Birks, J.B.; Pantos, E.; Hamilton, T. D. S. *Chem. Phys. Lett.* **1973**, *30*, 544–546.

(28) An apparent exception is the case of DMB in a solid O_2 matrix reported by Akimoto's group (ref 7a and b). A long-wavelength absorption tail extending to about 550 nm was noted. From irradiation with filtered Hg arc light it was concluded that the threshold to chemical reaction lies around 520 nm. Using tuned CW Ar ion laser light instead of filtered Hg arc radiation to excite DMB/O_2 matrices at 12 K, we have not been able to detect any reaction at 514, 488, or 458 nm (1 h at 500 mW cm^{-2} at each wavelength). However, the same photochemistry as reported by Akimoto was observed when irradiating the matrix with 355-nm laser light.

the excited charge-transfer state. Similarly, the onset of the DMB·O_2 charge-transfer absorption in non-zeolitic environments is at 400 nm, which also indicates a 12 000 cm^{-1} stabilization of the corresponding charge-transfer state in NaY.

This very strong stabilization of alkene·O_2 excited charge-transfer states must result from strong electrostatic interactions inside the supercage of NaY. The supercage framework carries a formal negative charge of 7 due to the presence of Al in the zeolite lattice. It is counterbalanced by the charges of seven Na^+ ions (NaY has the unit cell composition $Na_{56}(AlO_2)_{56}(SiO_2)_{136}$ with 8 supercages per unit cell).[20] The Na^+ ions are positioned inside the hexagonal cage (site S_I)[20] or inside the supercage (site S_{II} and site S_{III}).[20] There are four tetrahedrally arranged S_{II} sites and six octahedrally arranged S_{III} sites in each supercage.[29a] The cations in the supercage are little shielded electrically by the oxygens, and accepted models assign partial atomic charges of +1 to these sodium atoms and $-1/8$ to the framework oxygen atoms.[30] The alkene·O_2 ground-state complex is stabilized in the charged supercage mostly by ion-induced dipole interactions. Upon photoexcitation to the alkene$^+$·O_2^- charge-transfer state, these relatively weak interactions between the zeolite matrix and the reactants give way to far stronger and longer range Coulomb attractive interactions. Electrostatic field strengths even at distances between 2 and 4 Å from the wall or a Na^+ ion are on the order of one to several volts per angstrom.[29] Coulombic interaction of a positive and a negative unit charge even at a distance of 7 Å (corresponding to the radius of the supercage) would give rise to a 2-eV stabilization. Hence, one can readily envision a stabilization of the excited alkene$^+$·O_2^- charge-transfer state by one to several electronvolts, eV, depending on the position of the complex with respect to cage walls and Na^+ ions. The shorter wavelength onset of the reaction excitation spectrum in the case of the high-silica faujasite zeolite implies a 0.5 eV smaller stabilization of the excited charge-transfer state of DMB·O_2 compared to zeolite NaY. This is consistent with the fact that HSF is a nonionic matrix yet still carries negatively polarized oxygens.[31]

Red shifts (positive solvatochromism) of charge-transfer bands with increasing solvent polarity in the case of neutral donor–acceptor complexes in liquid solution have been observed but are of much lower magnitude.[32] Kochi has conducted studies on aromatic (donor)–pyridinium (acceptor) complexes in faujasitic zeolites and found that, in the case of these organic salts, charge-transfer bands are shifted relative to the solution phase but only modestly (10–30 nm).[33] The same holds for charge-transfer absorptions of transition metal complexes investigated by Dutta and co-workers.[34] Dutta has employed Taft-type empirical solvent parameters to characterize interactions in faujasitic zeolites as a function of the Si/Al ratio. Using a H-bonded anil system as a probe, it was found that the parameter α (describing the H-bond ability of the cage environment) is most important in this case.[35]

While it seems clear that, in the case of alkene$^+$·O_2^-, electrostatic interactions with the zeolite environment give rise to the 12 000-cm^{-1} (1.5-eV) stabilization of the charge-transfer state, quantum chemical modeling will be needed in order to obtain the details of these interactions.

Scheme 1

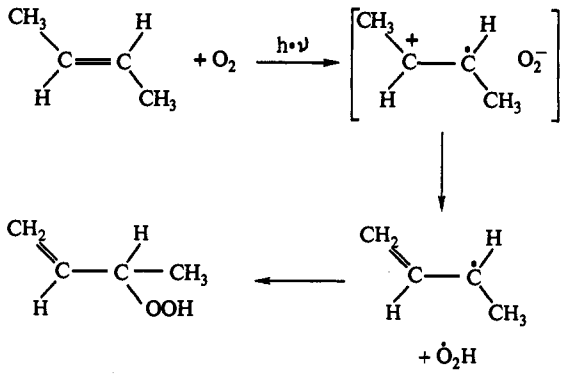

2. Mechanism of Photochemical Reaction. As described briefly in our preliminary report,[8] the most probable mechanism of the excited alkene·O_2 charge-transfer chemistry is deprotonation of the alkene to form an allyl radical and HO_2. Cage recombination of the radicals would generate the allylic hydroperoxide. This path is presented in Scheme 1 for the case of *trans*-2-butene + O_2. Alkene radical cations are known to be very strong acids.[36] We are not aware of any time-resolved measurements of proton-transfer rates involving small alkene radical cations. However, deprotonation rates of methyl-substituted naphthalene radical cations have been reported by Jones in his studies of excited charge-transfer state chemistry of naphthalene and cyclopolyene–chloranil complexes.[37,38] Rates were found to lie in the range of 10^6–10^7 s^{-1}.[37] Estimations of reaction quantum efficiencies based on diffuse reflectance measurements of the charge-transfer bands now in progress will allow us to assess how the competition between proton transfer and back electron transfer differs among the various alkenes. This will be reported in a forthcoming paper.[16] While hydroperoxide formation is the sole photochemical path in the case of *cis*- and *trans*-2-butene + O_2, single-photon-induced generation of acetone signals a second reaction channel in the case of DMB + O_2. This product is interpreted in terms of transient formation of dioxetane,[8] similar to the case of electron-transfer-sensitized photooxidation of olefins by dyes,[4] at semiconductor surfaces,[39] and UV-induced cleavage of phenylethenes in solution and on silica and alumina surfaces.[4b,6] The increased acetone yield at higher photolysis photon energies is attributed to the higher excess internal energy with which the transient dioxetane is formed.

The observed allylic hydroperoxides are the familiar 'ene' products of the reaction of $O_2(^1\Delta)$ with alkenes that possess allylic hydrogen.[3] Specifically, dye-sensitized singlet O_2 + DMB reaction gives 2,3-dimethyl-3-hydroperoxy-1-butene in high yield.[3a] *cis*- and *trans*-2-butene react with $O_2(^1\Delta)$ to give 3-hydroperoxy-1-butene, but at lower efficiency.[40] Ogilby has recently demonstrated by direct $^1\Delta \rightarrow {}^3\Sigma^-$ phosphorescence measurements that excitation of aliphatic and aromatic molecule·O_2 charge-transfer states leads to formation of singlet O_2.[41] Hence, a possible alternative to the mechanism proposed above is singlet oxygen generation via the excited charge-transfer state followed by reaction of $O_2(^1\Delta)$ with the alkene to yield allylic hydroperoxide. We can rule out, however, a substantial role of this path in our zeolite photochemistry for mainly two reasons.

(29) (a) Rabo, J. A.; Angell, C. L.; Kasai, P. H.; Schomaker, V. *Discuss. Faraday Soc.* **1966**, *41*, 328–349. (b) Huang, Y. Y.; Benson, J. E.; Boudart, M. *Ind. Eng. Chem. Fundam.* **1969**, *8*, 346–353. (c) Dempsey, E. In *Molecular Sieves*; Society of Chemical Industry: London, 1968; pp 293–305. (d) Spackman, M.A.; Weber, H. P. *J. Phys. Chem.* **1988**, *92*, 794–796.

(30) Bezus, A. G.; Kiselev, A. V.; Lopatkin, A. A.; Du, P. Q. *J. Chem. Soc., Faraday Trans. 2* **1978**, *74*, 367–379.

(31) Mortier, W. J. *J. Catal.* **1978**, *55*, 138–145.

(32) (a) Reichardt, C. *Solvent Effects in Organic Chemistry*; Verlag Chemie: Weinheim, Germany, 1979; p 195. (b) Dupire, S.; Mulindabyuma, J. M.; Nagy, J. B.; Nagy, O. B. *Tetrahedron* **1975**, *31*, 135–141.

(33) (a) Sankararaman, S.; Yoon, K. B.; Yabe, T.; Kochi, J. K. *J. Am. Chem. Soc.* **1991**, *113*, 1419–1421. (b) Yoon, K. B.; Kochi, J. K. *J. Phys. Chem.* **1991**, *95*, 3780–3790. (c) Yoon, K. B.; Kochi, J. K. *J. Am. Chem. Soc.* **1989**, *111*, 1128–1130.

(34) Turbeville, W.; Robins, D. S.; Dutta, P. K. *J. Phys. Chem.* **1992**, *96*, 5024–5029.

(35) Dutta, P. K.; Turbeville, W. *J. Phys. Chem.* **1991**, *95*, 4087–4092.

(36) (a) Anderson, D. R.; Bierbaum, V. M.; Depuy, C. H.; Grabowski, J. J. *Int. J. Mass Spectron Ion Phys.* **1983**, *52*, 65–94. (b) Hammerich, O.; Parker, V. D. *Adv. Phys. Org. Chem.* **1984**, *20*, 55–189.

(37) Jones, G., II; Mouli, N. *J. Phys. Chem.* **1988**, *92*, 7174–7177.

(38) Jones, G., II; Haney, W. A. *J. Phys. Chem.* **1986**, *90*, 5410–5414.

(39) Fox, M. A. *Acc. Chem. Res.* **1983**, *16*, 314–321.

(40) Shimizu, N.; Bartlett, P. D. *J. Am. Chem. Soc.* **1976**, *98*, 4193–4200.

(41) (a) Scurlock, R. D.; Ogilby, P. R. *J. Phys. Chem.* **1989**, *93*, 5493–5500. (b) Kristiansen, M.; Scurlock, R. D.; Iu, K. K.; Ogilby, P. R. *J. Phys. Chem.* **1991**, *95*, 5190–5197.

First, as Figure 9 shows, the hydroperoxide yields for 2-butene + O_2 and DMB + O_2 are similar if we take into account the shorter wavelength onset of the CH_3—CH=CH—CH_3 + O_2 reaction due to the higher ionization potential of 2-butene compared to DMB. On the basis of gas-phase and solution data, orders of magnitude lower yields are expected for the 2-butene + O_2 system if $O_2(^1\Delta)$ were involved. In these media, reaction rates of *cis*(*trans*)-2-butene + $O_2(^1\Delta)$ are over 2 (3) orders of magnitude smaller than that of the DMB + $O_2(^1\Delta)$ reaction.[42-44] Given the detection limit of our experiment, we would not have been able to observe any 2-butene + O_2 photoproduct if $O_2(^1\Delta)$ were principally involved. Second, in the case of the DMB + O_2 system, the photochemical branching between hydroperoxide and acetone changes abruptly in favor of acetone when zeolite NaY is replaced by high-silica faujasite. No such change in the branching between the two products is expected in the case of $O_2(^1\Delta)$ involvement because solvent polarity is known to have very little effect on the rate of singlet O_2 'ene' reactions.[4d,15,44] On the other hand, deprotonation is expected to be much less favored in the less polar HSF matrix. The mechanism presented in Scheme 1 accounts qualitatively for this observation. We conclude that deprotonation of the alkene moiety of the excited charge-transfer state is most probably the key step of the reaction mechanism.

It is interesting to note that in media in which the excited charge-transfer state is not stabilized (gas, solution, solid O_2), the reaction can only be induced by UV light. As a result, the chemistry is far less controlled. In solid O_2 at 10 K, for example, UV photochemistry of *trans*- or *cis*-2-butene + O_2 gives exclusively fragmentation products acetaldehyde, CO, CO_2, and O_3 along with extensive stereochemical scrambling of the reactant.[7b]

An intriguing aspect of the subsequent thermal reaction of 3-hydroperoxy-1-butene with excess *cis*- or *trans*-2-butene observed upon warm-up from −50 °C to room temperature is that it constitutes a case of uncatalyzed epoxidation of a small alkene by a hydroperoxide.[45] The epoxidation is completely stereospecific.

3. Mechanism of the Thermal DMB + O_2 Reaction. The main observation in the case of the thermal reaction between DMB and O_2 in zeolite NaY at 0 °C is that the products are completely different from those of the photochemical DMB + O_2 reaction at this same temperature. This indicates that the thermal reaction path is distinct from the photochemical one. The thermal reaction products in the zeolite have also nothing in common with those of thermal oxidation of DMB by O_2 in gas phase or solution. In the latter case, the hydroperoxides $(CH_3)_2C{=}C(CH_3)CH_2OOH$ and $CH_2{=}C(CH_3)$—$C(CH_3)_2OOH$ are among the principal primary products.[46] These emerge from reaction initiated by abstraction of methyl H. By contrast, the predominant product of the thermal reaction in NaY, pinacolone, suggests that O_2 attacks the alkene mainly at the C=C bond to form transient $(CH_3)_2\dot{C}$—$C(O\dot{O})(CH_3)_2$ biradical. We attribute this new thermal path to the enhanced role of the charge-transfer component in the ground electronic state[47] due to the strong electrostatic field of NaY. Elimination of O, or direct transfer to another DMB molecule may lead to $(CH_3)_2\dot{C}$—$C(\dot{O})(CH_3)_2$. 1,2-CH_3 migration under concurrent CO double-bond formation would yield pinacolone. In fact, $(CH_3)_3C$—C(=O)CH_3 is a major product of the thermal reaction of O atoms with DMB, a reaction that features the same transient $(CH_3)_2\dot{C}$—$C(\dot{O})(CH_3)_2$ biradical.[48] It is interesting to note that no 2,3-dimethyl-3-hydroperoxy-1-butene is produced along the thermal path. If the intermediate $(CH_3)_2\dot{C}$—$C(O\dot{O})(CH_3)_2$ is indeed formed, it would imply that intramolecular 1,5-H shift[49] is not competitive with O—O bond rupture in the zeolite matrix.

V. Conclusions

The main finding of this work is that alkene-O_2 excited charge-transfer states are strongly stabilized in zeolite NaY matrices. The stabilization is attributed to the very strong electrostatic interactions inside the zeolite cages. It allows us to access very low energy photooxygenation pathways, resulting in high product selectivity. This is best illustrated by the red-light-induced reaction of *cis*- or *trans*-2-butene with O_2, which gives allylic hydroperoxide as the sole product. In media that do not stabilize the excited charge-transfer state (gas, solution, solid O_2), the photoreaction can only be induced by UV light with the consequence that the chemistry is much less controlled.

Enhancement of the cage electrostatic field by substituting Na^+ by the smaller Li^+ or by bivalent cations (Ba^{2+} through Mg^{2+}) is expected to open up access to visible-light-induced oxygenation of important hydrocarbons such as propylene and small aromatics. Beyond offering an opportunity to exploit their strong electrostatic field, an important practical aspect of zeolite matrices is that they constitute a natural ambient-temperature environment for preparing and sustaining high concentrations of reactant collisional pairs. Excitation of collisional pairs with long-wavelength photons is an ideal way to access controlled low-energy pathways of bimolecular reactions.[50]

Acknowledgment. This work was supported by the Director, Office of Energy Research, Office of Basic Energy Sciences, Chemical Sciences Division of the U.S. Department of Energy, under Contract No. DE-AC03-76F00098.

(42) Ogryzlo, E. A. In ref 3a, p 50.
(43) Gollnick, K.; Kuhn, H. J. In ref 3a, pp 287–295.
(44) Hurst, J. R.; Schuster, G. B. *J. Am. Chem. Soc.* **1982**, *104*, 6854–6856.
(45) March, J. *Advanced Organic Chemistry*, 4th ed.; Wiley: New York, 1992; p 827.
(46) (a) Van Sickle, D. E.; Mayo, F. R.; Arluck, R. M.; Syz, M. G. *J. Am. Chem. Soc.* **1967**, *89*, 967–977. (b) Hession, M.; Jones, K.; Steiner, H. M. E. *J. Chem. Soc. A* **1971**, 350–360.
(47) (a) Turro, N. J.; Ramamurthy, V.; Liu, K. C.; Krebs, A.; Kemper, R. *J. Am. Chem. Soc.* **1976**, *98*, 6758–6768. (b) Yamaguchi, K. In *Singlet O_2*; Frimer, A. A., Ed.; CRC Press: Boca Raton, FL, 1985; Vol. 3, Part 2, pp 146, 147.
(48) Cvetanovic, R. J.; Singleton, D. L. *Rev. Chem. Intermed.* **1984**, *5*, 183–226.
(49) Reference 45, p 1067.
(50) (a) Frei, H. In *Vibrational Spectra and Structure*; Durig, J. R., Ed.; Elsevier: Amsterdam, The Netherlands, 1992; Vol. 20, pp 1–66. (b) Frei, H. *Chimia* **1991**, *45*, 175–190.